Extraction of Bridge Features from high-resolution InSAR Data and optical Images

Uwe Soergel
IPI Institute of Photogrammetry and GeoInformation
Leibniz Universität Hannover,
30167 Hannover, Germany

soergel@ipi.uni-hannover.de

Antje Thiele, Hermann Gross, Ulrich Thoennessen
FGAN-FOM Research Institute for Optronics and Pattern Recognition
76275 Ettlingen, Germany

Abstract— **Modern airborne SAR sensor systems provide geometric resolution in the order well below half a meter. By SAR Interferometry from pairs of such images DEM of the same grid size can be obtained. In data of this kind many features of urban objects become visible, which were beyond the scope of radar remote sensing only a few years ago. However, because of the side-looking SAR sensor principle, layover and occlusion issues inevitably arise in undulated terrain or urban areas. Therefore, SAR data are difficult to interpret even for senior human interpreters. Furthermore, the quality of the InSAR DEM may vary significantly depending on the local topography. In order to support interpretation SAR data are often analyzed using additional complementary information provided by maps or other remote sensing imagery. In this paper a fusion of high-resolution InSAR data and one aerial image is discussed for the example of a scene containing bridges that are core elements of infrastructure. The aims are improvement of the 3D visualization of the scene and the extraction of the main parameters of the bridges' geometry.**

I. INTRODUCTION

Synthetic aperture radar (SAR) has become a central remote sensing technique in the last two decades. Key features of SAR are its independency from weather conditions and time of day, because of the larger signal wavelength (usually 3 to 25 centimeters) compared to the visible spectrum respectively the active sensor principle. As a consequence, SAR is capable to gather data at any given time under the prerequisite a sensor is available. Operating space borne systems like ERS-2 and ENVISAT provide rather coarse spatial resolution (e.g. 25m grid on ground). The analysis of such imagery is often restricted to radiometric properties, e.g. mapping by land cover classification based on statistical pattern recognition techniques. The structure of settlement areas can usually be characterized in generalized manner only, e.g. for discrimination between inner city areas and suburbs. By SAR Interferometry (InSAR) digital elevation models (DEM) are derived from processing of couples of complex SAR images. Since the spatial spacing of the DEM is the same than the initial SAR imagery, the level of detail of such DEM derived from repeat-pass space-borne data is in general not dense enough for urban analysis. By means of time series analysis subsidence monitoring is possible with the Differential Interferometry and Persistent Scattering techniques [6]; the latter is especially feasible for urban scenes where many time-stable strong point scatterers are present.

In the case of time critical events like natural disasters SAR is useful due to its weather and time of day independency. Hence, disaster management [12] and damage assessment [20] in urban scenes are important applications of SAR. Because of the limited resolution of operational satellite systems, up to now the analysis was mostly restricted to medium scale products, e.g. for post-earthquake damage assessment [7], [24]. In contrast to short-time incidences like earthquakes, in the case of flooding, where the tidal peak may propagate along a river for several days, data may be gathered already during that event. This offers the opportunity to support the authorities with actual flood maps, which are useful to steer countermeasures preventing further damage and enabling humanitarian relief [1]. Due to climate change, flooding events of unfortunately even increasing devastation capability are more frequently observed posing a severe threat to many populated places of the earth [11].

The sensor evolution due to technical progress resulted in an impressive improvement of spatial resolution about one order of magnitude during the last decade. Upcoming civil satellite systems, for example TerraSAR-X [17], will achieve geometric resolution about two meters. Airborne experimental sensor systems are today capable to resolve objects in the decimeter scale in amplitude SAR data [5] while commercial systems, driven by private enterprises like Intermap [19], provide amplitude and interferometric SAR (InSAR) data over vast areas well below half a meter grid mesh size. Motivated by this development many efforts have been carried out to detect and reconstruct man-made objects from high-resolution SAR data only, for example for purposes of building recognition [8], [23] and road extraction [25].

But, the SAR technique has one principal drawback, namely the necessity of oblique viewing geometry, giving rise to undesired phenomena such as layover, occlusion, and multipath propagation [18] frequently observed in undulated terrain [14] and urban scenes [4]. Therefore, even high-resolution SAR is in general not the first choice for routine mapping targeting at urban scenes.

In order to circumvent limitations and improve results either multi-aspect SAR data are required [2], [23] or fusion of SAR imagery with data of different sources. Such complimentary data could be for example existing CAD vector data [21] or remote sensing imagery of other spectral domains provided by GIS. In the latter case the fusion with imagery from the visible domain is especially important, because such data is in many countries (including developing countries) available since map update relies often on high-resolution aerial orthophotos. Hence, it is a reasonable assumption that optical images are the most probable data source available for fusion, for example an aerial photograph from the archives could be used to support the interpretation of actual SAR data in the case of a time critical event.

Fusion of optical and SAR data was studied already intensively for satellite data [3], [10] or even airborne data with geometric resolution down to one meter [9]. Tupin and Roux [26] investigated radargrammetric 3D building reconstruction from a single SAR image of spatial grid better than one meter and one aerial image.

In this paper, fusion of one high-resolution InSAR data set and one aerial image is discussed. This is demonstrated for the example of a scene containing several bridges over water. Bridges are key elements of man-made infrastructure. Monitoring of these important connecting parts of the traffic network is vital for applications such as disaster management or in the context of political crisis, e.g. to evacuate inhabitants and to deliver goods and equipment. Aims of the approach are to smooth the noisy InSAR DEM data for example at water surfaces, to determine the water level, to derive key features of the bridge's geometry from the complementary data sources, and finally to generate an improved 3D visualization of the scene by data fusion. It is assumed that an aerial image is available for fusion with actual InSAR data. Special features of the appearance of bridges in InSAR data are exploited to determine the height of the bridge over water while the geometric extents of the bridge can be better estimated from the photo.

The paper is organized as follows. In Section 2 the typical appearance of high-resolution InSAR data containing bridges and water is discussed. Geometric constraints for the mapping of bridge structures into the SAR imagery are given. The fusion of the InSAR and optical data is presented in Section 3. This approach is demonstrated for InSAR data of spatial resolution better than 40 cm in range and even finer in azimuth direction.

II. INSAR DATA CONTAINING BRIDGES AND WATER SURFACES

The effects of water surfaces on InSAR data are discussed for the test data containing water canals and three bridges depicted in Figure 1 (a: magnitude, b: elevation, c: coherence). The single-pass X-band SAR data were acquired by the AeS sensor of Intermap Technologies, spatial data resolution is 38.5 cm in range and 18 cm in azimuth, illumination direction is from right to left, off nadir angle θ is approximately 43 degree.

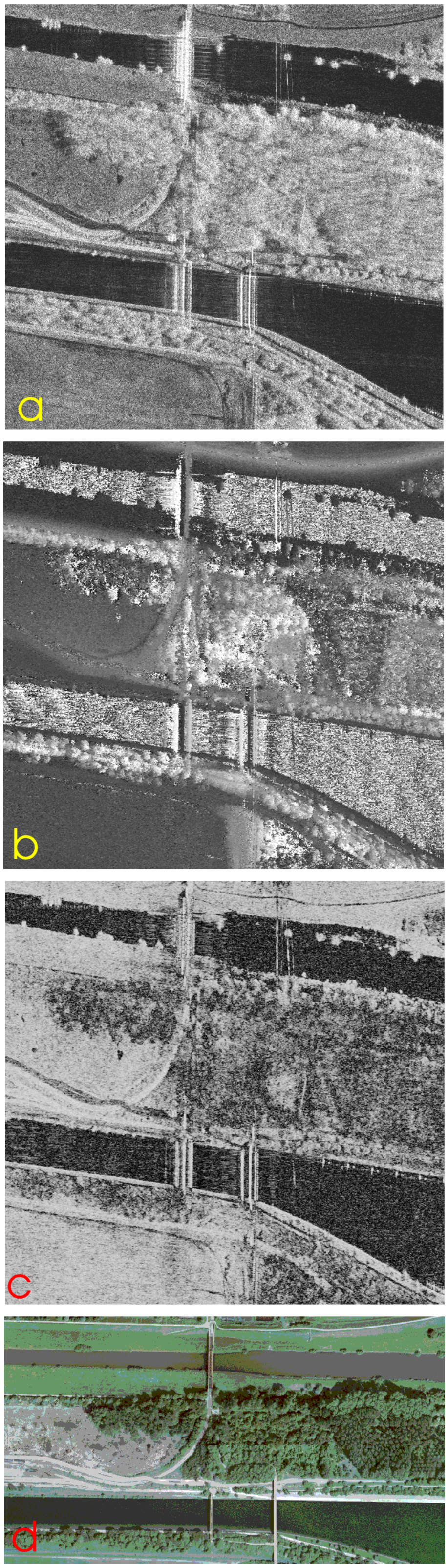

Figure 1. InSAR data sets with spatial resolution approximately 38 cm in range and 18 cm in azimuth, off-nadir angle 43 degree, SAR illumination direction (range) is always from right to left: a-c) magnitude, elevation (DEM), and coherence images of an interferogram showing three narrow bridges over water; d) aerial image of same area.

Calm water acts like a mirror to the oblique incoming SAR signal therefore most of the signal power is reflected away and almost no backscatter returns to the sensor. As a consequence, the signal to noise ratio (SNR) is poor, which leads to low mean interferometric coherence values at water locations and the coinciding InSAR elevation data are dominated by noise. Furthermore, if a river cuts a scene into two parts, phase-unwrapping algorithms might fail at that barrier. Other regions of poor InSAR elevation data quality arise from occlusion behind elevated objects, such as mountains, buildings and trees. In these areas the interferogram consists of noise only. Hence, in general pre-processing is required before the InSAR data can be transformed into the world coordinate system based on its own elevation values.

In order to demonstrate the effect of quite different local accuracy of the original InSAR elevation data without further artifacts caused by geocoding, the aerial image illustrated in Figure 1d was projected from the ground into the slant range geometry of the SAR data. This is shown in Figure 2, where the aerial image was superimposed on the InSAR elevation data in a 3D visualization of the scene. Due to low SNR, the image of the water areas resembles more to forests than to smooth surfaces. Furthermore, the bridges look strange in this visualization shown here based on the original DEM; the reason for this effect is discussed below in more detail.

Figure 2. Aerial image projected on original InSAR elevation data.

Assuming a zero mean noise model, the average of all InSAR elevation values over the entire water surface is expected to be a good estimate of the true water level. But, in the test data this was not the case, the elevation values were instead evenly distributed over the unambiguous elevation range of 22 meters, leading to a wrong estimate of about four meters from the average elevation compared to the reference.

However, it is possible to determine the water level by analysis of the images of the bridges in the SAR data. Furthermore, some features of the bridges' structure can be obtained from the InSAR images. Bridges over calm water illuminated not along their main orientation (i.e. the viewing direction has a significant vector component parallel to the course of the canal or river) may cause multiple images in SAR data. This will be discussed for the example of magnified images of the two bridges in the lower part of the scene and the principle sketch shown in Figure 3d.

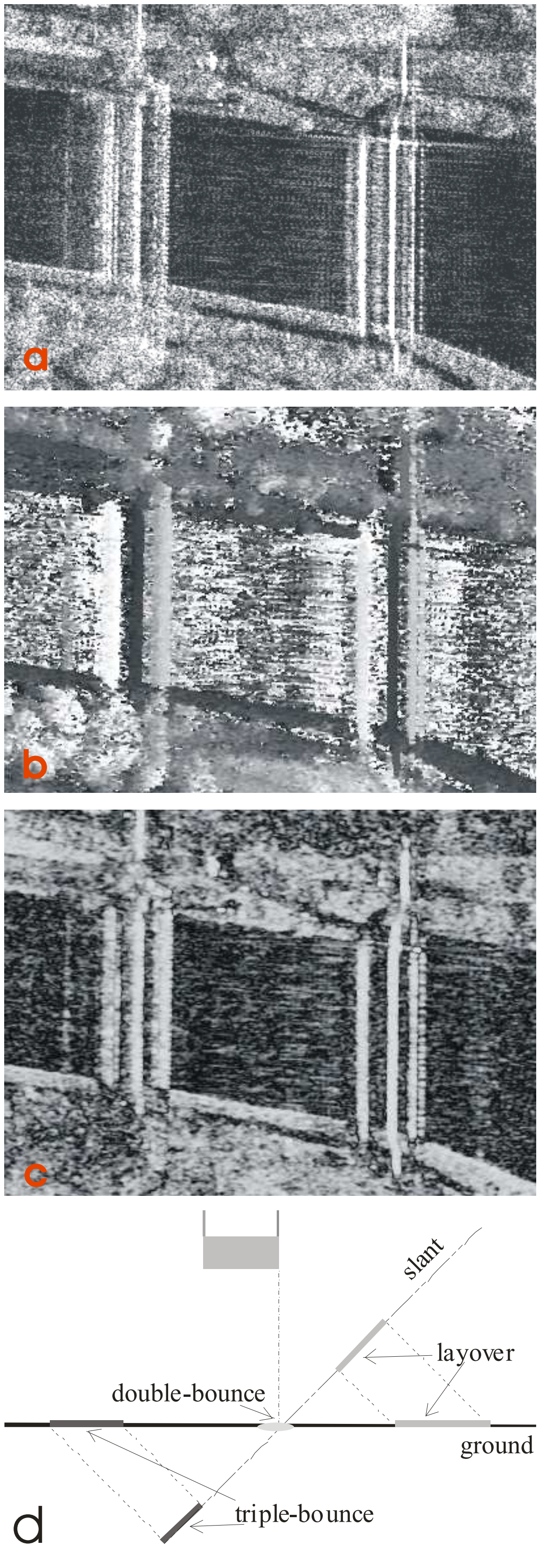

Figure 3. a-c) InSAR data: magnification of lower part of Figure 1 with two bridges; sketch explaining typical triple-stripe phenomenon.

Usually three subsequent parallel structures are observed at increasing range locations: first direct backscatter from the bridge (more precise: layover of bridge and water signal), followed by double-bounce reflection between bridge and water or vice versa, and finally triple reflection (water, lower parts of the bridge and water again). Often superstructure elements and piles are also visible [15]. Recently, it was demonstrated that in same cases in high-resolution SAR data additional multi-bounce signals of lower magnitude may show-up at even larger ranges, which are caused by pairs of back and forth scattering events between the bottom of the bridge and the water [13].

In SAR data of coarser resolution usually the three main structures appear as salient bright lines in sharp contrast to surrounding water surface [16]. From the ground range distance Δg_s of first to second or second to third stripe and off nadir angle θ the bridge height h can be estimated according to:

$$h = \Delta g_s / \tan\theta. \quad (1)$$

In SAR data of finer spatial sampling however the structures are not line-like anymore, but appear as stripes of considerable width, which has to be considered for geometric analysis. Additionally, in the case of InSAR data further information is available in form of interferometric elevation and coherence.

The mentioned triple-stripe structure is present again in the magnitude, elevation, and coherence images shown in Figure 3. Since the stripes are caused by complementing effects of different signal-runtime, they represent separate elevation levels.

Despite layover, the first stripe (here: the most right one) represents the height of the bridge body itself, because the layover signal is dominated from the bridge's contribution compared to the water contribution that is mainly scattered away. Due to the high resolution of the data some details of the bridge structures become visible. For example, in the case of the bridge on the right, even the signal from the main body of the bridge can be distinguished from the handrail that appears as dashed structure.

The second stripe is caused by double-bounce reflection occurring at the corner reflector spanned from smooth vertical bridge facets facing the sensor and the water surface. By theory all these double-bounce signal contributions should integrate into the range cell that coincides with the direct reflection or single-bounce backscatter path length from the nadir projection of the vertical bridge elements on the water surface. But, due to additional scattering events (e.g. at different vertical bridge construction elements) and non-perfect smoothness of bridge and water surface, the double-bounce signal is usually spread out some pixels around this point. The related elevation represents the true water level, because no matter how the actual signal path is, the runtime is always the same as that of a direct signal stemming from the footprint of the corner reflector on the water surface.

Very interesting is also the third bridge image (the most left one for each bridge) resulting from triple-bounce reflection between water, the lower bridge part, and water again. Because of the longer path length the signal is mapped to a position behind the true bridge location in range direction. Geometrically the origin of the signal seems to be a virtual bridge replica produced by mirroring the real bridge at the water surface. The interferometric elevation values of such stripes were in some cases far too high in the final DEM product, possibly due to folding upwards into the unambiguous phase range of 2π equivalent to 22m relative elevation difference here.

The height h of the bridge over the water level is an important feature for example in the case of flooding, in order to monitor if water level causes a threat to the bridge's structure, which might have impact on disaster management carried out by the local authorities. This height can be derived from the difference of the second stripe, which represents the true water level, and the first stripe giving the height of the bridge. Both stripes show high mean coherence values and because of their extent over several hundred pixels each, the related height estimates are robust. These relative measurements can be transferred into the absolute coordinate system using a single reference point. The results were compared to reference data: the average estimated height of the bridges main body over water surface of 11 meters in all three cases were correct with error smaller than half a meter. More details of the geometric constraints and an automatic approach for bridge extraction are given in [22].

III. FUSION OF INSAR AND OPTICAL DATA

As discussed in the previous section, it is possible to determine the height over water of the bridge, but, because of the multiple appearances of single bridges and dominant scattering occurring at pylons or superstructures, it is difficult to derive the outlines of the bridge from the SAR data. This can easily be done based on the aerial photo taken in nadir view. Here, the widths of the bridges were measured manually.

Using this information and because the true position of the bridge is known (it just starts at the double-bounce stripe) the InSAR elevation data can be corrected accordingly: a stripe of the measured width and average height replaces the original data at the bridge locations. Some additional processing steps are carried out to improve the DEM. The estimated water level is used to replace the noisy InSAR data at water surfaces. The water surfaces are detected by simply thresholding the amplitude image in order to extract dark regions. This threshold is derived from histogram analysis, looking for the first significant minimum. By subsequent morphological processing holes are filled and small darker regions, which might be caused e.g. from asphalt surfaces or shadow, are filtered out. Furthermore, the remaining InSAR elevation data are smoothed by averaging in a 5x5 window using the related coherence values as weight. Assuming the water surfaces to represent the lowest local elevation level, smaller elevation values are replaced by more consistent values taken from the vicinity. The result of this process is illustrated in Figure 4a.

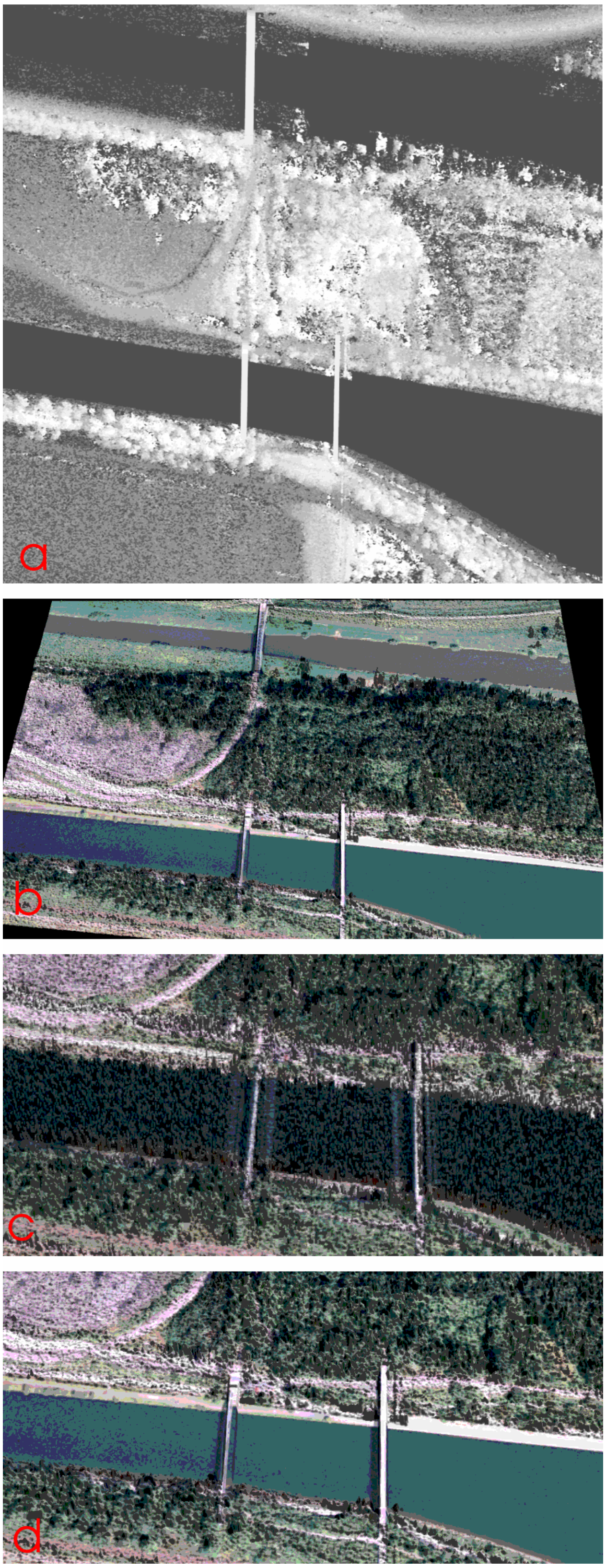

Figure 4. a) InSAR DEM after smoothing; b) aerial image projected on processed InSAR elevation data; c) detail of Figure 2; d) same area after processing.

Compared to the original data shown in Figure 1b the improvement is obvious. Again, the aerial image was superimposed on the slant range DEM, the impression of the 3D structure depicted in Figure 4b is now more realistic than before. The water surfaces appear now smooth and the triple bridge structures have vanished. This result seems to be a more suitable basis for further studies than the original data, no matter if interactive or automatic analysis is targeted.

For better comparison, the scene part covering the lower two bridges is shown in Figure 4 c,d, once overlaid on the original DEM and in the other case overlaid on the smoothed DEM. In the improved result still a minor artifact is visible; the left bridge seems not to fit perfectly, instead it is shifted by a few pixels. Such effects can be eliminated by further fine adjustment steps, which were not carried out at the time being, but will be investigated in the future.

IV. Conclusion

Modern SAR sensors achieve such high spatial resolution that even rather small bridges are mapped with considerable level of detail. Besides the higher resolution, another advantage of airborne systems compared to space borne sensors is flexibility, which is of importance for purposes such as disaster management. It is possible to derive key features of bridges like the height of the bridge over the actual water level from data of this quality. Furthermore, even details such as handrails become visible. All three kinds of interferometric data channels, namely magnitude, elevation and coherence images are useful for the analysis of the geometry of man-made objects in the scene. However, due to the side-looking sensor principle of SAR data of this kind is difficult to interpret even for experts.

Fusion with optical data allows obtaining further features for example the width of bridges. Combining the information about the bridge location and structure taken from the complimentary data sources, the InSAR DEM can be improved. After additional smoothing steps, the 3D visualization of the aerial imagery on the InSAR DEM gives far better impression of the scene topography.

In this paper first results of a long term study were published. Based on these results, there is still potential for further improvements. Up to now, only the average bridge height is considered for analysis, neglecting any super- and substructures. In future work detail structures of this kind shall be considered as well in subsequent fine analysis steps incorporating features detected both in the SAR and the optical data.

References

[1] Bach, H., Appel, F., Fellah, K., de Fraipont, P, 2005. Application of flood monitoring from satellite for insurances, Procedings of IGARSS, unpaginated CD-ROM, 4p.

[2] Bolter, R., 2001. Buildings from SAR: detection and reconstruction of buildings from multiple view high resolution interferometric SAR data, PhD thesis, University of Graz, Austria.

[3] Dare P., and Dowman I., 2000. A new Approach to Automatic Feature Based Registration of SAR and Spot Images. International Archives of Photogrammetry and Remote Sensing, Vol. 33, B2, pp. 125-130.

[4] Dong, Y., Forster, B., Ticehurst, C., 1997. Radar backscatter analysis for urban environments, Int. Journal of Remote Sensing, Vol. 18, No. 6, pp. 1351-1364.

[5] Ender, J.H.G., and Brenner, A.R., 2003. PAMIR - a wideband phased array SAR/MTI system, IEE Proceedings - Radar, Sonar, Navigation, Vol. 150, No. 3, pp. 165-172.

[6] Ferretti, A., Prati, C., and Rocca, F., 2000. Nonlinear subsidence rate estimation using permanent scatterers in differential SAR interferometry. IEEE Transactions on Geoscience and Remote Sensing, Vol. 38, No. 5, pp. 2202-2212.

[7] Funning, G.J., Parsons, B., Wright, T.J., Jackson, J.A., and Fielding, E.J., 2005. Surface displacements and source parameters of the 2003 Bam (Iran) earthquake from Envisat advanced synthetic aperature radar imagery, Journal of Geophysical Research, Vol. 110, No. B9, B09406, 23 p.

[8] Gamba, P., Houshmand, B., Saccani, M.: “Detection and extraction of buildings from interferometric SAR data,” In: IEEE Transactions on Geoscience and Remote Sensing, Vol. 38, No. 1, Part 2, pp. 611–617, 2000.

[9] Hellwich, O., Reigber, A., Lehmann, H., 2002. Sensor and data fusion contest: Test imagery to compare and combine airborne SAR and optical sensors for mapping. International Archives of Photogrammetry and Remote Sensing, Vol. 34 Part 3B, pp. 75-78.

[10] Hong D.H., and Schowengerdt R., 2005. A Robust Technique for Precise Registration of Radar and Optical Satellite Images. Photogrammetric Eng. & Remote Sensing, Vol. 71, No. 5, 585-593.

[11] International Charter Space and Major Disasters: list of recent floodings: http://www.disasterscharter.org/new_e.html flooding of river Elbe, Germany and Czechia, April 2006: http://www.disasterscharter.org/disasters/CALLID_116_e.html

[12] Kakumoto, S., Hatayama, M., Kameda, H., Taniguchi, T., 1997. Development of disaster management spatial information system, Proceedings of GIS, pp. 595-598.

[13] Lee, J. S., Ainsworth, T. L., Krogager, E., Boerner, W. M., 2006. Polarimetric Analysis of Radar Signature ofa Manmade Structure, Proceedings of IGARSS, unpaginated CD-ROM, 4p.

[14] Meier, E., Frei, U., and Nuesch, D., 1993. Precise terrain corrected geocoded images, SAR geocoding: data and systems, (G. Schreier, editor) Wichmann Verlag, Karlsruhe, Germany, pp. 173-185.

[15] Raney, R. K., 1998. Radar Fundamentals: Technical Perspective. In Henderson, Floyd M., and Anthony J. Lewis, ed., Manual of Remote Sensing 3rd Edition: Principles and Applications of Imaging Radar, Vol. 2. American Society for Photogrammetry and Remote Sensing, 1998, pp 9-130.

[16] Robalo, J. and Lichtenegger, J., 1999. ERS-SAR Images a bridge, ESA, Earth Oberservation Quarterly, December 1999, pp. 7-10 (see also: http://esapub.esrin.esa.it/eoq/eoq64/bridge.pdf).

[17] Roth, A., Eineder, M., Schaettler, B., 2003. SAR interferometry with TerraSAR-X, ESA Workshop Fringe.

[18] Schreier, G., 1993. Geometrical properties of SAR images, SAR geocoding: data and systems, (G. Schreier, editor) Wichmann Verlag, Karlsruhe, Germany, pp. 103-134.

[19] Schwaebisch, M., and Moreira, J., 1999. The High Resolution Airborne Interferometric SAR AeS-1. Proceedings of the Fourth International Airborne Remote Sensing Conference and Exhibition, Ottawa, Canada, pp. 540-547.

[20] Shinozuka, M., Ghanem, R., Houshmand, B., Mansuri, B., 2000. Damage detection in urban areas by SAR imagery, Journal of Engineering Mechanics, Vol. 126, No. 7, pp. 769-777.

[21] Soergel, U., Schulz, K., Thoennessen, U., Stilla, U., 2005. Integration of 3D Data in SAR Mission Planning and Image Interpretation in Urban Areas. Information Fusion, Elsevier B.V., Vol. 6, No. 4, pp. 301-310.

[22] Soergel, U., Cadario, E., Gross, H., Thiele, A., Thoennessen U., 2006. Bridge Detection in multi-aspect high-resolution Interferometric SAR Data. Proceedings of 6th European conference on synthetic aperture radar, EUSAR, unpaginated CD-ROM, 4p.

[23] Soergel, U., Thoennessen, U., and Stilla, U., 2003. Reconstruction of Buildings from Interferometric SAR Data of built-up Areas. Proc. of PIA, International Archives of Photogrammetry and Remote Sensing, Vol. 34, Part 3/W8, pp. 59-64.

[24] Takeuchi, S., Suga, Y., Yonezawa, C., Chen, C.H., 2000. Detection of urban disaster using InSAR - a case study for the 1999 great Taiwan earthquake, Proceedings of IGARSS, unpaginated CD-ROM, 4p.

[25] Tupin, F., Maitre, H., Mangin, J-F., Nicolas, J-M,. Pechersky, E., 1998. Detection of linear features in SAR images: application to road network extraction, IEEE Transactions on Geoscience and Remote Sensing, Vol. 36, No. 2, pp. 434-453.

[26] Tupin, F., and Roux, M., 2004. Markov Random Field on Region Adjacency Graph for the Fusion of SAR and Optical Data in Radargrammetric Applications, IEEE Transactions on Geoscience and Remote Sensing, Vol. 43, No. 8, pp. 1920-1928.

1-4244-0712-5/07/$20.00 ©2007 IEEE.